

Since F_{ox} is unbounded for equatorial intersections, ϵ_{ox} is degenerate, and all states are to be counted, the formulation proposed in Ref. 1 is inconsistent and should be revised. The length $0 \leq \ell \leq D_0$ defines the time from initial oxidizer particle exposure at the burning surface. Therefore, it uniquely defines all states. Consequently, replacing $F_{ox} d\epsilon_{ox}$ with $F_{ox,\ell} d\ell$ eliminates the aforementioned inconsistencies. This yields

$$\dot{m}_{ox} = N \int_0^{D_0} F_{ox,\ell} \epsilon_{ox} \int_{\epsilon_f}^{\infty} m_{ox} F_j d\epsilon_f d\ell \quad (16)$$

Equation (16) should replace Eq. (7) of Ref. 1. Extension of monodisperse distribution functions to polydisperse situations is treated in Ref. 2.

References

- ¹Glick, R.L., "On Statistical Analysis of Composite Solid Propellant Combustion," *AIAA Journal*, Vol. 12, Mar. 1974, pp. 384-385.
- ²Glick, R.L., "Statistical Analysis of Non-Metallized Composite Solid Propellant Combustion," CPIA Publication 243, Vol. 1, Dec. 1973, pp. 157-184.
- ³Beckstead, M.W., Derr, R.L., and Price, C.F., "A Model of Solid Propellant Combustion Based on Multiple Flames," *AIAA Journal*, Vol. 8, Dec. 1970, pp. 2200-2207.
- ⁴Dole, M., *Introduction to Statistical Thermodynamics*, Prentice-Hall, Inc., Englewood Cliffs, N.J., 1954, pp. 48-60.
- ⁵Dallavalle, J.M., *Micromeritics*, Pitman Publishing Company, New York, 1948, pp. 123-143.

†As noted previously, $F_{ox,\ell} = I/D_0$ for monodisperse situations.

Free-Interface Methods of Substructure Coupling for Dynamic Analysis

Roy R. Craig Jr.* and Ching-Jone Chang†
The University of Texas, Austin, Tex.

Introduction

SUBSTRUCTURE coupling methods have been developed in order to reduce the number of coordinates in a dynamic analysis of a complex structure, to permit analysis and design of different portions of a structure to proceed independently, and to permit testing of various portions of a structure to be done independently. References 1 and 2 survey most of the currently available methods with Ref. 2 providing numerical comparisons of the accuracy of eigenvalues obtained by a number of the methods. Substructure coupling methods can be classified as fixed-interface methods, free-interface methods, or hybrid methods, depending upon whether the mode shapes used to define substructure coordinates are obtained with the interface coordinates fixed, free, or a combination of the two. As noted by Benfield, et al.² the fixed-interface methods have been found to produce the best accuracy, while the free-interface methods of Hou and Goldmann produced the poorest accuracy.

Although accuracy, or rate of convergence, is an important criterion to be used in selecting a substructure coupling method, two other important criteria are: substructure independence and test compatibility. None of the methods sur-

veyed in Ref. 2 satisfies all three of the aforementioned criteria.

Several authors have suggested augmenting substructure normal modes in order to improve the convergence of free-interface methods.³⁻⁶ In the present Note a substructure coupling method employing free-interface substructure normal modes supplemented by "reduced flexibility" will be presented. The basic ideas for representing the substructures are contained in the works of MacNeal⁴ and Rubin.⁶ The purpose of the present Note is to present a discussion of substructure coupling based on the improved substructure model and to present numerical results comparing the present method, which will be referred to as MacNeal's method, with Hou's method. To simplify presentation of the method here, the substructure equations are developed first for constrained substructures. Then the equations representing substructures with rigid-body modes are presented. Finally, the equations for coupling of substructures are developed, and examples are given.

Substructure Equations

Since the primary concern of this Note is to describe a substructure coupling method for use in calculating system modes and frequencies, only the equations of undamped vibration will be considered. For a given substructure, these may be written in the form

$$\begin{bmatrix} m_{ii} & m_{ij} \\ m_{ji} & m_{jj} \end{bmatrix} \begin{Bmatrix} \ddot{x}_i \\ \ddot{x}_j \end{Bmatrix} + \begin{bmatrix} k_{ii} & k_{ij} \\ k_{ji} & k_{jj} \end{bmatrix} \begin{Bmatrix} x_i \\ x_j \end{Bmatrix} = \begin{Bmatrix} 0 \\ f_j \end{Bmatrix} \quad (1)$$

where x_j is the set of junction (interface) coordinates, x_i is the set of interior coordinates, and f_j contains the forces transmitted to the substructure through junction coordinates. The free-interface modes are determined by the eigenvalue equation

$$[k - \lambda_\alpha^2 m] \phi_\alpha = 0 \quad (2)$$

The modes will be assumed to be normalized so that

$$\phi_\alpha^T m \phi_\alpha = 1, \quad \phi_\alpha^T k \phi_\alpha = \lambda_\alpha^2 \quad (3)$$

and collected to form a modal matrix Φ .

A coordinate transformation relating physical coordinates, x , to modal coordinates p is given by

$$x = \Phi p \equiv \Phi_k p_k + \Phi_a p_a \quad (4)$$

where $\Phi_k p_k$ is the contribution of modes which are kept. The contribution $\Phi_a p_a$ will be replaced by an approximation.

When Eq. (4) is substituted into Eq. (1) there results a set of n equations of the form

$$\ddot{p}_\alpha + \lambda_\alpha^2 p_\alpha = \phi_{j\alpha}^T f_j \quad (5)$$

If harmonic motion is assumed, i.e., $p = \bar{p} \cos \omega t$, etc., Eqs. (4) and (5) may be combined to give

$$\begin{aligned} \bar{x} = \sum_{\alpha=1}^n \phi_\alpha \left(\frac{\phi_{j\alpha}^T \bar{f}_j}{\lambda_\alpha^2 - \omega^2} \right) &\doteq \sum_{\alpha=1}^{n_k} \phi_\alpha \left(\frac{\phi_{j\alpha}^T \bar{f}_j}{\lambda_\alpha^2 - \omega^2} \right) \\ &+ \sum_{\alpha=n_k+1}^n \phi_\alpha \left(\frac{\phi_{j\alpha}^T \bar{f}_j}{\lambda_\alpha^2} \right) \end{aligned} \quad (6)$$

The last series represents the "residual flexibility" of modes not explicitly kept. This can be obtained by subtracting from the flexibility matrix, $G = k^{-1}$, the contribution due to kept modes. Then Eq. (6) may be written as

$$\bar{x} = \Phi_k \bar{p}_k + G^a \bar{f} \quad (7)$$

Received Nov. 20, 1975; revision received Aug. 3, 1976. This work was supported by NASA Grant NSG 1001.

Index categories: Structural Dynamic Analysis; Aircraft Vibration; LV/M Dynamics, Uncontrolled.

*Associate Professor, Aerospace Engineering and Engineering Mechanics. Member AIAA.

†Graduate Student, Engineering Mechanics.

where

$$G^a = G - \Phi_k \Lambda_k^{-1} \Phi_k^T \quad (8)$$

Finally, Eqs. (5) and (7) lead to the primary equations representing a substructure, namely

$$[-\omega^2 I + \Lambda_k] \bar{p}_k = \Phi_{jk}^T \bar{f}_j \quad (9)$$

and

$$\bar{x}_j = \Phi_{jk} \bar{p}_k + G_{jj}^a \bar{f}_j \quad (10)$$

If a substructure has rigid-body degrees of freedom, the static flexibility matrix, $G = k^{-1}$, does not exist, and an alternative formulation is required. MacNeal⁴ proposed the following procedure. Let the orthonormalized rigid-body modes and flexible-body modes form the modal matrices Φ_r and Φ_f , respectively. Then

$$x = \Phi_r p_r + \Phi_f p_f \quad (11)$$

The resulting rigid-body equations of motion are

$$\ddot{p}_r = \Phi_r^T f \quad (12)$$

The rigid body inertia forces are given by

$$f_I = -m \ddot{x}_r = -m \Phi_r \Phi_r^T f \quad (13)$$

Hence, under the action of applied forces f , the substructure is subjected to an equilibrated force system given by

$$f_f = f + f_I = [I - m \Phi_r \Phi_r^T] f \equiv A f \quad (14)$$

To determine the pseudo-static flexible-body displacement due to f_f it is necessary to determine the displacement relative to some arbitrary statically-determinate constraint and then to remove any rigid-body displacements from this relative displacement. Let G^c be the flexibility matrix relative to the imposed constraints (including rows and columns of zeros at the constraint degrees-of-freedom). Then

$$x_f = G f \quad (15)$$

where G is now given by

$$G = A^T G^c A \quad (16)$$

This expression for G is used in Eq. (8) when the substructure has rigid-body degrees-of-freedom. Then Φ_k must contain the rigid-body modes.

Coupling of Substructures

Let two substructures, A and B , be joined at a common interface. The compatibility of displacements and equilibrium of forces at the interface are expressed by the equations

$$\bar{x}_{jA} = \bar{x}_{jB} \quad (17)$$

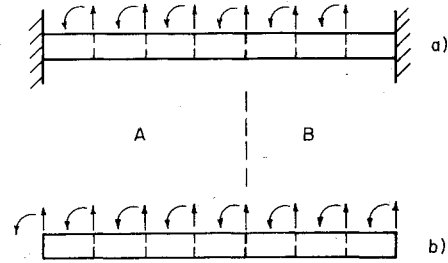


Fig. 1 Example two-substructure beams.

$$\bar{f}_{jA} = -\bar{f}_{jB} \quad (18)$$

If Eq. (10) is written for each substructure and Eqs. (17) and (18) are employed, the following expression for \bar{f}_{jA} is obtained

$$\bar{f}_{jA} = K_{jj} (\Phi_{jkB} \bar{p}_{kB} - \Phi_{jKA} \bar{p}_{kA}) \quad (19)$$

where

$$k_{jj} \equiv (G_{jjA}^a + G_{jjB}^a)^{-1} \quad (20)$$

Equation (9) may now be written for each substructure, with Eqs. (18) and (19) used to express \bar{f}_{jA} and \bar{f}_{jB} in terms of \bar{p}_{kA} and \bar{p}_{kB} . Then the following system equation is obtained.

$$\begin{bmatrix} K_{AA} & K_{AB} \\ K_{BA} & K_{BB} \end{bmatrix} \begin{Bmatrix} \bar{p}_{kA} \\ \bar{p}_{kB} \end{Bmatrix} = \omega^2 \begin{bmatrix} I_{AA} & 0 \\ 0 & I_{BB} \end{bmatrix} \begin{Bmatrix} \bar{p}_{kA} \\ \bar{p}_{kB} \end{Bmatrix} \quad (21)$$

where

$$\begin{aligned} K_{AA} &= \Lambda_{kA} + \Phi_{jKA}^T K_{jj} \Phi_{jKA} \\ K_{AB} &= K_{BA}^T = -\Phi_{jKA}^T K_{jj} \Phi_{jKB} \\ K_{BB} &= \Lambda_{kB} + \Phi_{jKB}^T K_{jj} \Phi_{jKB} \end{aligned} \quad (22)$$

Note that the final system coordinates are a combination of the kept modal coordinates of the two substructures, but all interface coordinates have been reduced out. Also note that the only information required to form the matrices of Eqs. (22), beyond information on the kept modes, is G_{jjA} and G_{jjB} . Hence, there is some promise that this method will prove to be quite compatible with currently feasible test procedures. Two brief examples are presented below to show the significant improvement in the present method as compared to Hou's method.

Examples

Figure 1 shows two beam configurations studied. In Table 1 the frequencies of a two-substructure clamped-clamped beam, as obtained by MacNeal's method, are compared with results obtained by Hou's method. In Table 2 similar results are presented for a two-substructure free-free beam.

Table 1 Frequencies of a two-substructure clamped-clamped beam

Elastic mode number	$n_A = 4, n_B = 3$		$n_A = 6, n_B = 4$		$n_A = 4, n_B = 3$		Exact
	MacNeal $\omega^2 \times 10^{-1}$	% error	MacNeal $\omega^2 \times 10^{-1}$	% error	Hou $\omega^2 \times 10^{-1}$	% error	$\omega^2 \times 10^{-1}$
1	0.00020855	0.00	0.00020854	0.00	0.00024825	19.04	0.00020854
2	0.00158782	0.02	0.00158760	0.00	0.00172805	8.85	0.00158754
3	0.00614521	0.14	0.00613799	0.02	0.00723442	17.89	0.00613670
4	0.01707075	0.54	0.01699774	0.11	0.02294540	35.13	0.01697985
5	0.03890897	0.68	0.03866336	0.04	0.04195877	8.57	0.03864799
6	0.07975906	5.47	0.07613860	0.68	0.07562475
7	0.40279307	x	0.16425283	0.48	0.16346229

Table 2 Frequencies of a two-substructure free-free beam

Elastic mode number	$n_A = 5, n_B = 4$		$n_A = 5, n_B = 4$		Exact $\omega^2 \times 10^{-1}$
	MacNeal $\omega^2 \times 10^{-1}$	% error	MacNeal $\omega^2 \times 10^{-1}$	% error	
1	0.00020855	0.00	0.00028069	34.60	0.00020854
2	0.00158753	0.02	0.00175287	10.44	0.00158720
3	0.00613810	0.14	0.00720175	17.49	0.00612967
4	0.01700570	0.55	0.02282519	34.96	0.01691298
5	0.03852031	0.69	0.04155454	8.62	0.03825621
6	0.07837021	5.52	0.07427024
7	0.39281608	x	0.15736511

Conclusions

The incorporation of residual flexibility into the formulation of a free-interface substructure coupling procedure is easily accomplished and produces a very significant improvement in the accuracy of system frequencies.

References

- ¹Hurty, W. C., "Introduction to Modal Synthesis Techniques," *Synthesis of Vibrating Systems*, ASME, Nov. 1971.
- ²Benfield, W. A., Bodley, C. S., and Morosow, G., "Modal Synthesis Methods," *Symposium on Substructure Testing and Synthesis*, NASA Marshall Space Flight Center, Aug. 1972.
- ³Bamford, R. M., "A Modal Combination Program for Dynamic Analysis of Structures," Jet Propulsion Lab., Pasadena, Calif., Tech. Memo 33-290, July 1967.
- ⁴MacNeal, R. H., "A Hybrid Method of Component Mode Synthesis," *Journal of Computers*, Vol. 1, No. 4, Dec. 1971, pp. 581-601.
- ⁵Klosterman, A. L., "On the Experimental Determination and Use of Modal Representations of Dynamic Characteristics," University of Cincinnati, Ph.D. Dissertation, 1971.
- ⁶Rubin, S., "Improved Component-Mode Representation for Structural Dynamic Analysis," *AIAA Journal*, Vol. 13, Aug. 1975, pp. 995-1006.

Free Flight Measurements of Catastrophic Water Drop Breakup

W. G. Reinecke* and W. L. McKay†
AVCO Systems Division, Wilmington, Mass.

To verify that the definition of catastrophic water drop breakup, which is based on x-ray and shadow images of the drops in the shock tube,¹⁻⁴ corresponds to the elimination of the drops' potential for erosion in flight, we conducted a free flight drop breakup and impact experiment in the Avco Rain and Dust Erosion Facility (RADEF).⁵ The RADEF is a ballistic range in which material samples are flown through rain, dust, or ice environments at speeds up to 15,000 fps, suffer multiple impact erosion, and are subsequently decelerated and recovered to measure erosion damage and crater morphology. In the verification tests a single monodisperse drop generator of the type described in Ref. 5 was used. The drop

Received July 12, 1976; revision received Aug. 30, 1976. Work supported by Elastomers and Coatings Branch, Nonmetallic Materials Division, Air Force Materials Lab. under Contracts F33615-74-C-5143 and -5149.

Index categories: Multiphase Flows; Hypervelocity Impact.

*Senior Consulting Scientist. Associate Fellow AIAA.

†Senior Staff Scientist.

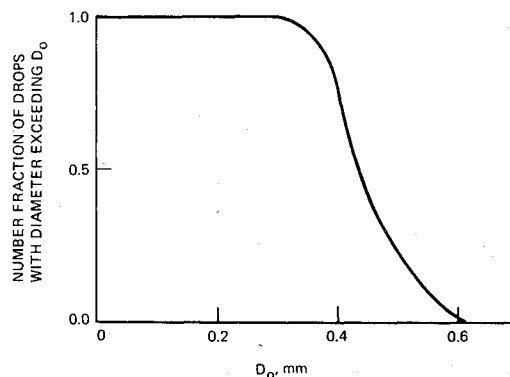


Fig. 1 Cumulative drop number fraction vs water drop diameter.

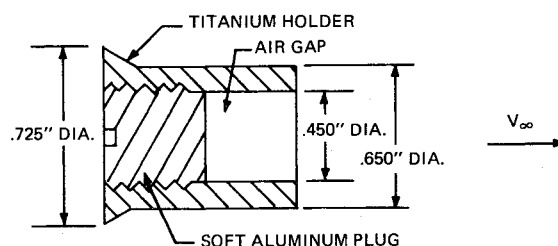


Fig. 2 Cross section of ballistic range water drop breakup and impact model.

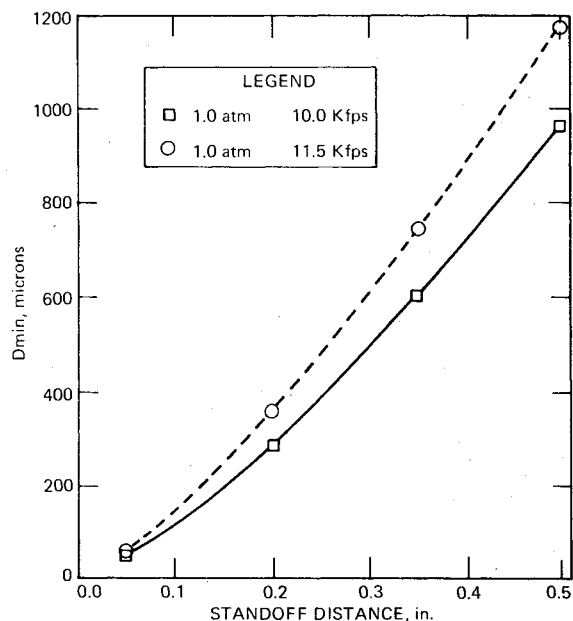


Fig. 3 Initial diameter of smallest drop reaching surface obtained from correlations of shock tube data.

size distribution was obtained from photographs of the generated drop streams. From these photographs, we can calculate the number fraction of drops with diameter exceeding any given diameter. This curve is shown in Fig. 1.

Since the two stage light gas gun in the RADEF cannot launch models larger than 0.8 inches in diameter at hypervelocities, it was necessary to fire recessed models through the rain field in order to achieve effective shock standoff distances large enough to shatter drops of the size produced by the generator. At hypersonic speeds and when viewed in the frame of reference of the undisturbed drops, there is only a small variation in aerodynamic conditions between the con-